지능구조물과 ASTROS*를 이용한 플러터 제어

Control of Flutter using ASTROS* with Smart Structures

김종선*, 남창호**

Jong-Sun Kim* and Changho Nam**

요 약

최근에 통합 설계 최적화 프로그램인 ASTROS*와 Aeroservoelasticity(ASE)모듈에 지능구조물의 해석 모듈을 통합하는 연구가 수행되었다. 통합된 소프트웨어를 이용해 플러터 억제 시스템을 설계하는 연구를 F-16모델을 이용해 수행하였으며 능동 제어 시스템을 위하여 신경망을 이용한 제어기가 설계되었다. 압전작동기에 의해 발생한 변형을 고려하기 위해 지능구조물 모듈은 ASTROS*내의 열응력 해석 모듈을 개량하여 개발되었으며 ASE내에서 조종면을 이용한 입력과 압전작동기를 이용한 입력의 상호 호환성을 가능하게 하였다. 수치 예를 통해 개발된 제어시스템이 플러터속도를 증가시키는 데 효과적임을 보였다.

Abstract

Recent development of a smart structures module and its successful integration with a multidisciplinary design optimization software ASTROS* and an Aeroservoelasticity module is presented. A modeled F-16 wing using piezoelectric actuators is used as an example to demonstrate the integrated software capability to design a flutter suppression system. For an active control design, neural network based controller is used for this study. A smart structures module is developed by modifying the existing thermal loads module in ASTROS* in order to include the effects of the induced strain due to piezoelectric actuation. The control surface/piezoelectric equivalence model principle is developed, which ensures the interchangeability between the control surface force input and the piezoelectric force input to the Aeroservoelasticity modules in ASTROS*. The results show that the developed controller can increase the flutter speed.

I. Introduction

In recent years, considerable interest has directed toward application of smart structures to control the static and dynamic aeroelastic responses for rotary-and fixed-wing aircraft [1],[2]. The application of the use of smart structures for aeroelastic control has been proposed, and a simple wind tunnel test for active flutter suppression via piezoelectric (PZT) actuators has also shown some promising results [3]. The application of these materials as actuators in flutter suppression has been examined in Refs [4]~[6]. The authors used optimization-techniques to find the best geometry of the PZT actuators for flutter suppression. Nam and Kim [7] used self-sensing PZT actuators for

* 한국항공대학교 항공우주 및 기계공학부(School of Aerospace and Mechanical Engineering, Hankuk Aviation Univ.)

· 논문번호 : 2001-1-10
· 접수일자 : 2001년 6월 15일

flutter suppression of a plate modeled wing. They also predicted the electric power required for aeroelastic control. Heeg et al. [8] conducted a wind tunnel test for flutter suppression using a swept wing model. They found that the materials are capable of suppressing flutter in the model. The prediction of electric power consumption may be an important factor for the real applications in aeroelastic control [9], [10]. It was found that the induced strain actuated control system might be used for aeroelastic control with less power and energy. However, in-depth study of predicting power requirements for aeroelastic control appears to be very limited.

For aeroelastic control, the selection of smart actuators requires a systematic parametric study of the best possible PZT and/or Shape Memory Alloy (SMA) combinations. Further, the total effort should amount to find their optimized size and location on a wing surface along with their integration with the wing structure. Such an effort would require tedious parametric study, which can only be conducted effectively through a multidisciplinary design and optimization (MDO) methodology. In this study, we adopt an MDO software system ASTROS*, previously developed by AFRL[11] and further integrated and maintained by ZONA Technology (ZONA) [12],[14]. ASTROS stands for Automated Structural Optimization System, which is a proven engineering design/analysis software including vast scope of aerospace disciplines that impact a structural design. We will further elaborate on ASTROS* in the following section. On the other hand, to formulate and make the smart-structure algorithm compatible with ASTROS* is not altogether a trivial task. The present paper present our recent development of a smart structure module and its integration with ASTROS* and the Aeroservoelasticity (ASE) module. To validate the developed software, we apply the smart structure module in conjunction with ASTROS* and ASE module for active flutter suppression of a modeled F-16 wing using PZT actuators.

Recently, the neural network-based control system, which uses a neural network embedded within a model predictive control framework, was applied for active wing flutter suppression [15], [16]. A neural network-based adaptive controller was also used to the buffet alleviation on scale model aircraft with twin vertical tails using both distributed piezoelectric and conventional rudder actuation [17]. They reduced up to 30% and 12% of the rms values in the first and second vibration modes, respectively, but they used SISO (single-input-single-output) model rather than MIMO (multi-input-multi-output) model. The use of neural networks to mimic the behavior of a modified LQG controller that is applicable to nonlinear aeroelastic systems was developed and applied to the helicopter rotor blade by Ku and Hajela [18]. They used the LQG controller as a feedback controller and the neural network as the feedforward compensator for the unmodeled nonlinear dynamics. In this paper, an alternative neuro control strategy, which has the advantage of the LQG controller at a given air speed as well as the adaptive controller for changes in operating conditions is applied to suppress the flutter.

Ⅱ. Modelling

2-1 ASTROS* and ASE Modules

ASTROS is a finite element based procedure tailored for the preliminary design of aerospace structures[11]. As such, it includes flexibility and generality in multiple discipline integration. For aircraft, spacecraft or missile design, the unique attributes of ASTROS lie in its savings in design effort and time, improvement in flight performance

and reduction in structural weight. In principle, ASTROS was aimed at the effective multidisciplinary interactions between aerodynamics, aeroelasticity, structures and other modules. For structural analysis, ASTROS has both statics and normal modes capabilities, and is based on the NASTRAN style input format for its finite element methodology. For optimization, ASTROS adopts Vanderplatts method of feasible directions [19]. Other analysis modules in ASTROS include the sensitivity analysis, aeroelastic analysis, control response and aerodynamic modules.

Under contracts with AFRL, ZONA has further developed ASTROS* through the integration of a unified steady/unsteady, wing-body aerodynamic module for all Mach numbers (the ZAERO module) and an aeroservoelastic module (ASE module) into the system [12]~[14]. Thus, ASTROS* is named after the integration of ASTROS with the ZAERO module and ASTROS*/ASE is named after the integration of ASTROS* with the ASE module. Recently, a Smart Structures (SS) module and a Trim module have been developed for ASTROS* (see Fig. 1).

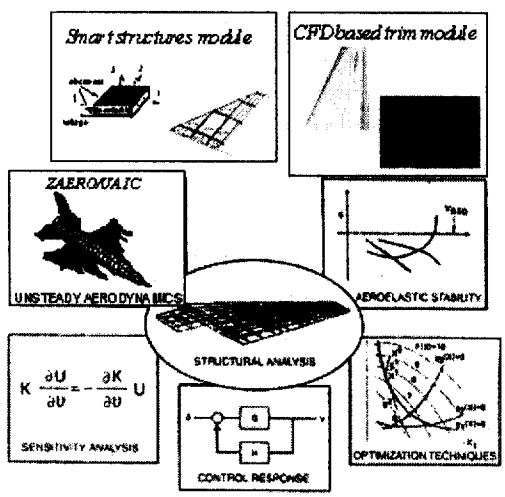

Fig. 1. ASTROS*+Smart Structure/CFD Based Trim Modules.

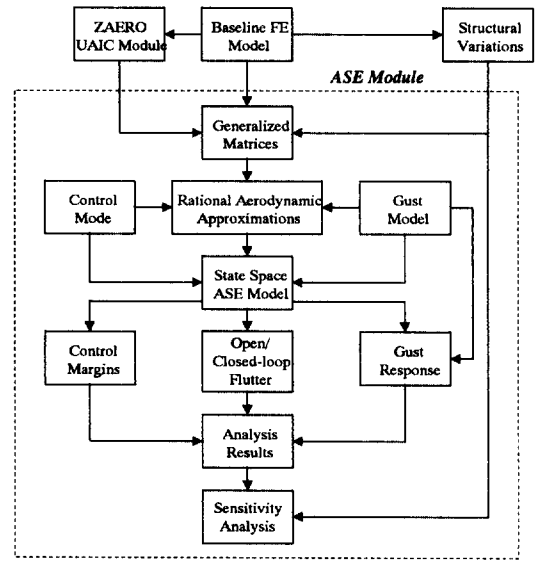

Fig. 2. ASE Module Flow Chart.

The ASE module facilitates the inclusion of multi-input multi-output (MIMO) control system effects on the dynamic stability and response in multidisciplinary analysis in design/optimization (see Fig. 2). The ASE module is based on state-space formulations. The structure is represented by a set of baseline normal modes serving as generalized coordinates. The unsteady aerodynamic forces are represented by minimum-state rational approximations [20] of the ZAERO module generated transcendental frequency domain generalized force coefficient matrices. The control system is represented by a state-space realization of a user-defined series of polynomial transfer functions. A gust filter is defined such that a white-noise input produces an approximation of either Drydens or von Karmans power spectral density of atmospheric continuous gusts. The stability analysis and constraints are based on root-loci curves, Nyquist curves and transfer-function singular values in the frequency domain. The gust response analysis and sensitivities are based on the stochastic Lyapunov formulation. There are several options for the

reduction of the order of the state-space equations. These options allow a combination of modal truncation, static residualization and dynamic residualization. The ASE module is applicable to open loop as well as closed loop systems.

2-2 Formulation of Smart Structures/ASE Modules

In order to use PZT actuators, it is assumed that wing has the segmented PZT actuators set which are attached at the top and bottom of the wing surface. It is also assumed that the opposite electric field is applied to the actuators set so as to create a pure bending moment for the aeroelastic control. When a voltage creates an electric field in the piezoelectric material, it will strain in three directions [21]

$$\varepsilon_{induced} = d_{ij}\frac{V_{II}}{t_P} \tag{1}$$

The constant measuring the strains per unit electric field are denoted as d_{ij} and measures the strain in the i direction due to a unit electric field applied in the j direction. V_{II} is the applied control voltage and t_P is thickness of piezoelectric materials. These induced strains are analogous to "thermal loads" that produce stress in the restrained structures

$$\varepsilon_{TEMP} = \alpha_{ij}\,\Delta T \tag{2}$$

where α_{ij} is the thermal expansion coefficient and $\triangle T$ is the temperature change. The close similarity between the PZT induced strain and the thermal load induced strain suggests that the formulation of thermal load computation in the finite element method can be adopted to compute the PZT induced strain. In fact, the ASTROS* smart structures module for PZT actuators is developed by modifying an existing thermal loads module in the ASTROS*, where the thermal expansion coefficient α_{ij} and the temperature change ΔT is replaced by d_{ij} and V_{Pt}/t_P. Similarly, the induced smart actuator strain/stress of SMA can also be converted into the actuation forces in ASTROS* with smart structures module[22].

In order to include the effects of the induced strain due to PZT actuation, a smart structures module is developed by modifying the existing thermal loads module in ASTROS*. The thermal-PZT/SMA equivalence model enables the modifications of the thermal stress module to accommodate the smart structures module in ASTROS*. The control surface (CS)/ PZT/ SMA equivalence model principle ensures the interchangeability between the CS force input and the PZT/ SMA force input to the ASE modules in ASTROS*. Aerodynamic forces due to control surface modes can be expressed as

$$\{F_c\} = [AIC]\{\varphi_c\} \tag{3}$$

where {AIC} is the aerodynamic forces coefficient matrix, $\{\varphi_c\}$ is the control surface mode defined at aerodynamic grid. Similarly, aerodynamic forces due to PZT/SMA modes are expressed as

$$\{F_p\} = [AIC][SPLINE]\{\varphi_P\} \tag{4}$$

where $\{\varphi_P\}$ is the PZT/SMA mode defined at structural finite element grid. It is noted that the variables, [AIC], [SPLINE], $\{\varphi_c\}$, and $\{\varphi_P\}$ are all existing data entities in ASTROS*. Therefore, $\{F_c\}$ and $\{F_P\}$ are interchangeable inputs to ASE module, whereas ASE module requires no modification for PZT/SMA control application.

2-3 Aeroservoelasticity (ASE) Module

The equations of motion for aeroservoelastic analysis can be written as

$$[M_s]\{\ddot{q}\}+[C_s]\{\dot{q}\}+[K_s]\{q\}+[M_c]\{\ddot{\delta}_c\}$$
$$=[Q_a]\{q\}+[Q_c]\{\delta_c\}+[Q_p]\{V_p\}$$
$$+[Q_G]\frac{w_G}{V}=q_d\left([A_d]\{q\}+[A_c]\{\delta_c\}\right.$$
$$\left.+[A_p]\{V_p\}+[A_G]\frac{w_G}{V}\right) \quad (5)$$

where $\{q\}$ are the generalized modal coordinates, q_d is the dynamic pressure. The matrices $[Q_a]$, $[Q_c]$, $[Q_p]$ and $[Q_G]$ are the generalized aerodynamic forces due to flexible modes, control surfaces mode, PZT mode and gust, respectively.

The aerodynamic forces are approximated as the transfer functions of the Laplace variable by a least square procedure in order to define the aeroservoelastic equations of motion in a linear time invariant state-space form. In the ASE module, we adopt the minimum state method [20] that approximates the unsteady aerodynamic forces in the following form.

$$[A_{ap}] =[A_qA_cA_pA_G]$$
$$=[\overline{P_0}]+[\overline{P_1}]s'+[\overline{P_2}]s'^2$$
$$+[\overline{D}]([I]s'-[\overline{R}])^{-1}[\overline{E}]s' \quad (6)$$

where $\overline{P_i}=[P_qP_cP_pP_G]_i$, $s'=ik=i\omega b/V$ $=sb/V$ and s is the Laplace variable, k is the reduced frequency, b is the semi-chord and V is the airspeed. The subscripts q, c, p and G indicate elastic, control surface, PZT and gust modes, respectively. In minimum state method, the augmented aerodynamic state is defined as follows

$$\{x_a\}=(s'[I]-[\overline{R}])^{-1}[E_qE_cE_pE_G]\begin{Bmatrix} q \\ \delta_c \\ V_p \\ w_G \end{Bmatrix} \quad (7)$$

Here, P_{G2} is set to zero to avoid $\ddot{w}_G$ term in the following state equation. Therefore,

$$[A_G]=[P_{G0}]+[P_{G1}]s'+[\overline{D}]([I]s'$$
$$-[\overline{R}])^{-1}[\overline{E}_G]s' \quad (8)$$

The control surfaces/PZT actuator transfer functions can be expressed in a state space form as follows.

$$\{\dot{x_c}\}=[A_c]\{x_c\}+\{B_c\}\delta_{command}$$
$$\{u_s\}=[C_c]\{x_c\} \quad (9)$$

The gust state space model is included for random gust response calculations. The vertical gust is modeled by a second order Dryden model:

$$\frac{w_g}{w}=\sigma_{wg}\frac{\sqrt{\frac{3V}{L}}\left(s+\frac{V}{L\sqrt{3}}\right)}{\left[s+\frac{V}{L}\right]^2} \quad (10)$$

where σ_{wg} is the root-mean square value of the gust velocity, L is the characteristic gust length and V is the airspeed. When the low pass filter is included, the state space equation of the gust is expressed as follows

$$\{\dot{x_g}\}=[A_g]\{x_g\}+\{B_g\}w$$
$$\{w_G\}=[C_g]\{x_g\} \quad (11)$$

By including the gust dynamics system and the actuator system, the following state space aeroservoelastic model is obtained.

$$\{\dot{x}\}=[A]\{x\}+[B]\{u\}+\{B_w\}w$$
$$\{y\}=[C]\{x\} \quad (12)$$

where $\{x\}=\left[q^T\ \dot{q}^T\ x_a^T\ x_c^T\ x_g^T\right]^T$, {y} is the output vector.

Ⅲ. Control Design

3-1 LQG Controller Design at Specific Airspeed

Since the system dynamics is a function of the air speed, it is necessary to build a set of the linearized state space model with respect to the air speed, V. In order to apply the neural net based control scheme, the continuous time model is discretized using zero-order hold method with sampling frequency, f_s. The discrete time state space model can be written in the following form

$$\begin{aligned}\{x\ (k+1)\} &= [A(V_i)]\{x(k)\} \\ &+ [B(V_i)]\{u(k)\} + \{w(k)\}\{y(k)\} \\ &= [C(V_i)]\{x(k)\} + \{v(k)\} \\ &i = 1, 2, \ldots, n_v \end{aligned} \tag{13}$$

where $\{x(k), u(k)\}$ and $\{y(k)\}$ represent the state, input and output vectors, respectively, and the matrices $[A(V_i)]$, $[zB(V_i)]$ and $[C(V_i)]$ are the system, input and measurement matrices for the air speed of V_i, respectively. n_v is the number of specific air speed. The disturbance $\{w(k)\}$ and sensor noise $\{v(k)\}$ are both assumed to be stationary, zero mean, Gaussian white, and to have covariance matrices satisfying

$$\begin{aligned} &E[\{w(k)\}\{w(l)\}^T] = [W]\ \delta(l-k) \\ &\text{and}\quad E[\{v(k)\}\{v(l)\}^T] = [V]\ \delta(l-k) \\ &E[\{w(k)\}\{v(l)\}^T] = 0 \end{aligned} \tag{14}$$

where $E[\cdot]$ denotes the expected value, δ denotes the Kronecker delta, and $[W]$ and $[V]$ represent the intensities of the disturbance and the sensor noise, and are assumed to be positive definite.

As a first step, a set of Linear Quadratic Gaussian(LQG) controllers are designed at each specific air speed condition as follows

$$\begin{aligned}\{u\ (k)\} &= -[K(V_i)]\{\hat{x}(k)\} \\ \{\hat{x}(k+1)\} &= [A(V_i)]\{\hat{x}(k)\} \\ &+ [B(V_i)]\{u(k)\} + [H(V_i)][\{y(k)\} \\ &- [C(V_i)]\{\hat{x}(k)\}] \end{aligned} \tag{15}$$

where $\{\hat{x}\}$ denotes the estimated state and $[K]$, $[H]$ are the gain matrtix, Karman filter gain matrix, respectively. The control input can be determined subject to minimize the performance index which is expressed as follows:

$$\begin{aligned} J = E\Big\{ &\sum_{k=1}^{\infty} [\{x(k)\}^T [Q]\{x(k)\} \\ &+ \{u(k)\}^T [R]\{u(k)\}] \Big\} \end{aligned} \tag{16}$$

where $[Q]$ is positive semi-definite and $[R]$ is positive definite matrices, respectively. The optimal feedback gain matrix $[K]$ and the Kalman filter gain matrix $[H]$ are obtained from the control and filter Riccati equations, respectively.

3-2 Neural Network Controller

When the operating conditions such as the air speed change, the controller has to be redesigned for the non-adaptive linear control system. The input-output relations of the LQG controller are used as the data for training the neural network.

The neural network that used for controller is a Multi-Layer-Perceptron (MLP) trained with back-propagation. This type of neural network is a universal approximator, and able to learn any function to any degree of accuracy [23]. Feedback from the sensor output is digitized and fed into the inputs of the neural network and passed through a digital tapped-delay-line for past time steps. A similar process is used for feeding the current and past controls into the network inputs. In order to account the air speed variant characteristics, air

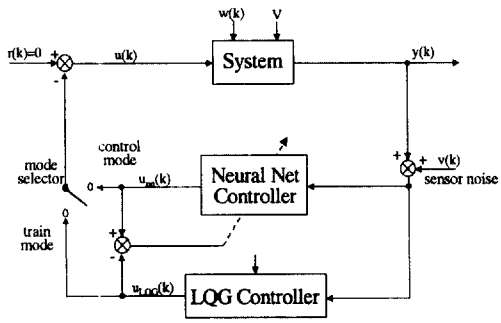

Fig. 3. Block diagram of flutter suppression system.

speed V, is included as an additional input to the network.

In Fig. 3, a neural net based control system is depicted. In this figure, each circle, or node, represent a single neuron. The output from the network is compared to the output of the corresponding LQG controller when the mode selector is at the train mode, and any difference between the two is backpropageted through the network to modify its learning parameters. The problem of finding a suitable set of neural net control parameters that approximates the LQG controller is solved using error back-propagation algorithm. The discrete time model of neural network as shown in Fig. 4 can be described by the following nonlinear difference equation

$$\{u_{NN}(k)\} = f[\{u_{NN}(k-1)\},\ \{y(k)\},\ \{y(k-1)\},\ V]$$

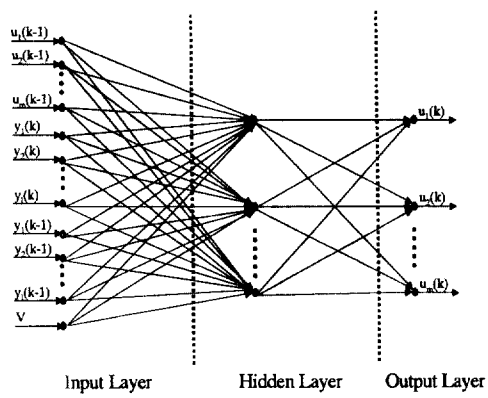

Fig. 4. Neural network plant model.

The parameters of feedforward networks are usually trained so as to minimize the following cost function

$$E = \sum_{i=1}^{n_o}\Big\{ \sum_{j=1}^{k} [\{u_{LQG}(j)\} - \{u_{NN}(j)\}]^T \quad (17)$$

$$[\{u_{LQG}(j)\} - \{u_{NN}(j)\}]\Big\}_i \quad (18)$$

where $\{u_{LQG}(j)\}$ and $\{u_{NN}(j)\}$ are the input vectors of LQG controller and neural network controller at sampling instant j, respectively. The Levenberg-Marquardt algorithm is used to minimize the defined cost function and obtain the next control input. After a neural network has been trained for varying the air speed, the mode selector is toggled to the control mode as shown in Fig. 3. Although the initial training time for a network may be long, it can be performed during off hours without much involvement of the designer. In order to properly train a neural network, it is important that the inputs to the network cover the range of possible values in terms of frequency. Addition of random signals as the reference may be useful for that purpose.

Ⅳ. Application Example - F-16 Smart Wing

A modeled F-16 smart wing is used as an example model to design control system for flutter suppression. Fig. 5(a) and (b) show the finite element and aerodynamic models of F-16 modeled wing [24]. The FEM model contains 86 grid points.

Total 62 membrane (CQDMEM/CTRMEM) element are used for modeling wing skin, 361 shear (CSHEAR) element for ribs and spars, and 111 rod (CROD) element for sparcaps and shear webs. The ZAERO module in ASTROS* is used to compute unsteady aerodynamic forces at Mach 0.9.

Total seven PZT actuator sets are used for the

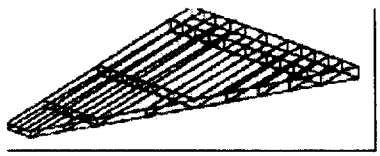

(a) Finite Element Model

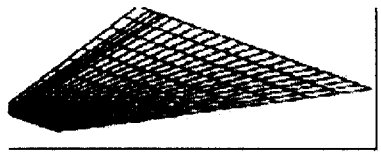

(b) Aerodynamic Model

Fig. 5. Finite Element and Aerodynamic Models of a Modeled F-16 Wing.

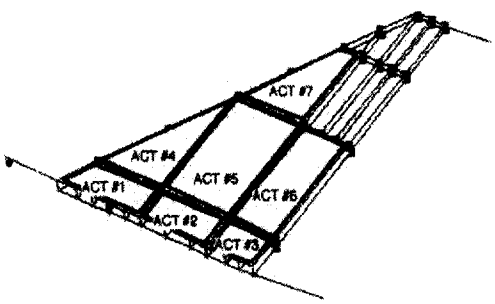

Fig. 6. Modeled Wing with 7 Sets of PZT Actuators.

aeroservoelastic control (see Fig. 6). Fig. 7 indicates the typical control mode shapes due to PZT actuations. Aerodynamic forces due to seven PZT modes are calculated and transformed into time domain in ASTROS*. After vibration analysis, a modal reduction is performed using the first seven elastic modes (see Fig. 8). The resulting state space model is 45th-order : These are seven displacement modes, seven rate modes, ten aerodynamic states due to minimum state approximation, and three actuator states for each PZT actuator due to minimum state approximation.

An open loop flutter analysis is conducted using ASTROS*. Fig 9 shows the open loop flutter analysis results. The open loop flutter of this model occurs around 1043 ft/sec, at Mach 0.9 and flutter frequency is 19.9 Hz. As shown in the figure.

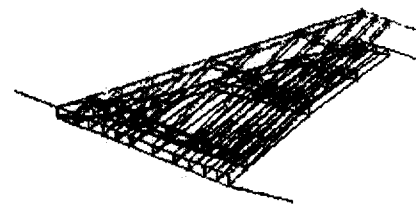

(a) Actuator No. 1

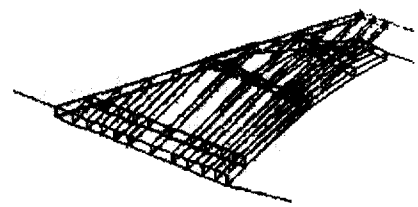

(b) Actuator No. 7

Fig. 7. Control Mode Shapes due to PZT Actuation(PZT Actuator no. 1 and 7).

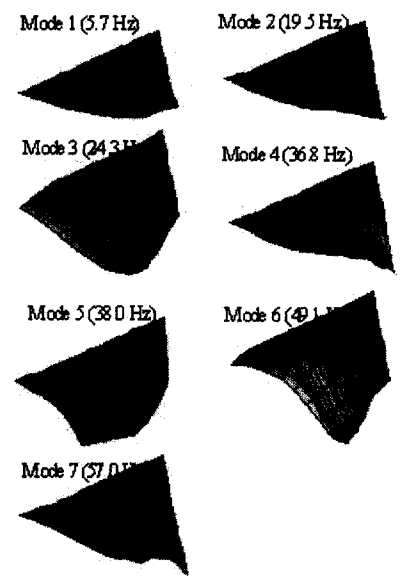

Fig. 8. Natural Frequencies and Mode Shapes of a F-16 Modeled wing.

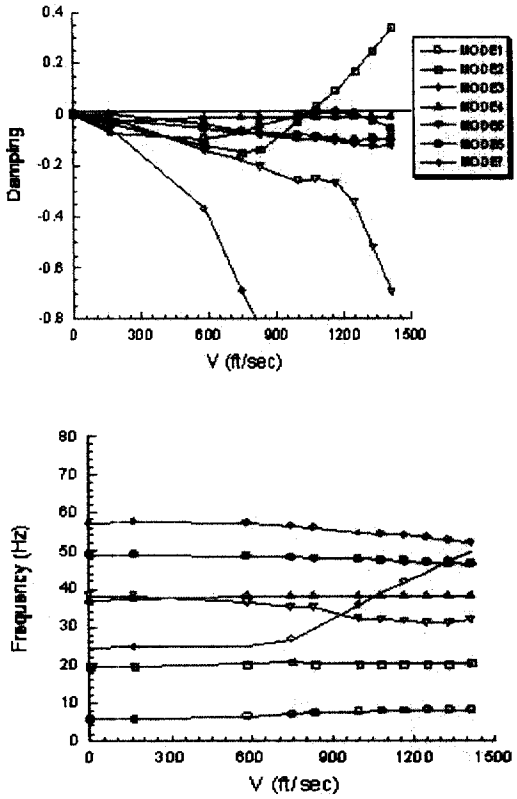

Fig. 9. Open Loop Flutter Analysis Results of a F-16 Modeled Wing.

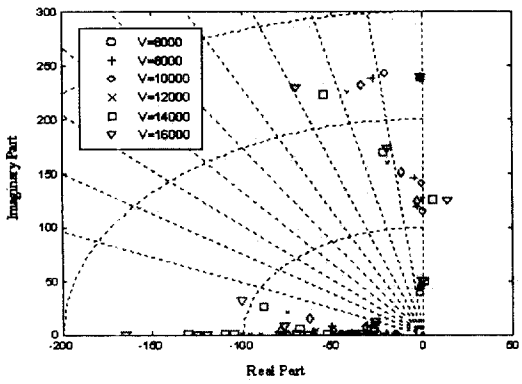

Fig. 10. Open loop eigenvalues of the system at the various airspeed.

second mode of the open-loop system becomes unstable. With this system model an active control

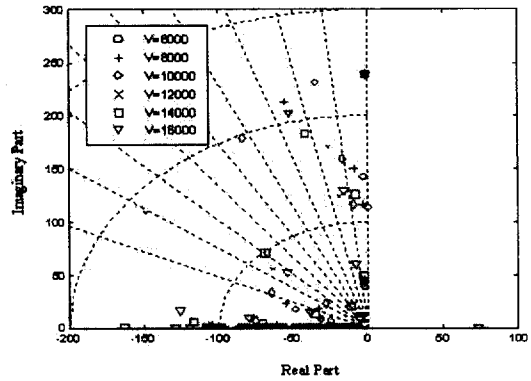

Fig. 11. Closed loop eigenvalues of the system at the various airspeed

system is designed by using LQG for flutter suppression. The design airspeed is set to be V= 1,166 ft/sec, Mach=0.9. Figs. 10 and 11 show the open loop and the closed loop eigenvalues of the system when LQG is used to design an active control system for flutter suppression at the design airspeed of 14000 in/sec. The design result shows that the closed loop system is stable up to 16000 in/sec. Using LQG design results and design airspeed, the neural net is trained for flutter suppression.

As described in the previous section, in order to design an active control system using neural network, a set of LQG controller are designed at each specific airspeed and the obtained data are used to train the neural network system. Fig. 12 contains the control system design results. Figures show the responses of the closed loop system (a and b) and the control input (c and d) which are the control voltage applied to the actuators. For the comparison, LQG results are also plotted in the figure. The results show that the system designed by neural network gives a better settling time and requires a less control input compared with those obtained by using LQG controller.

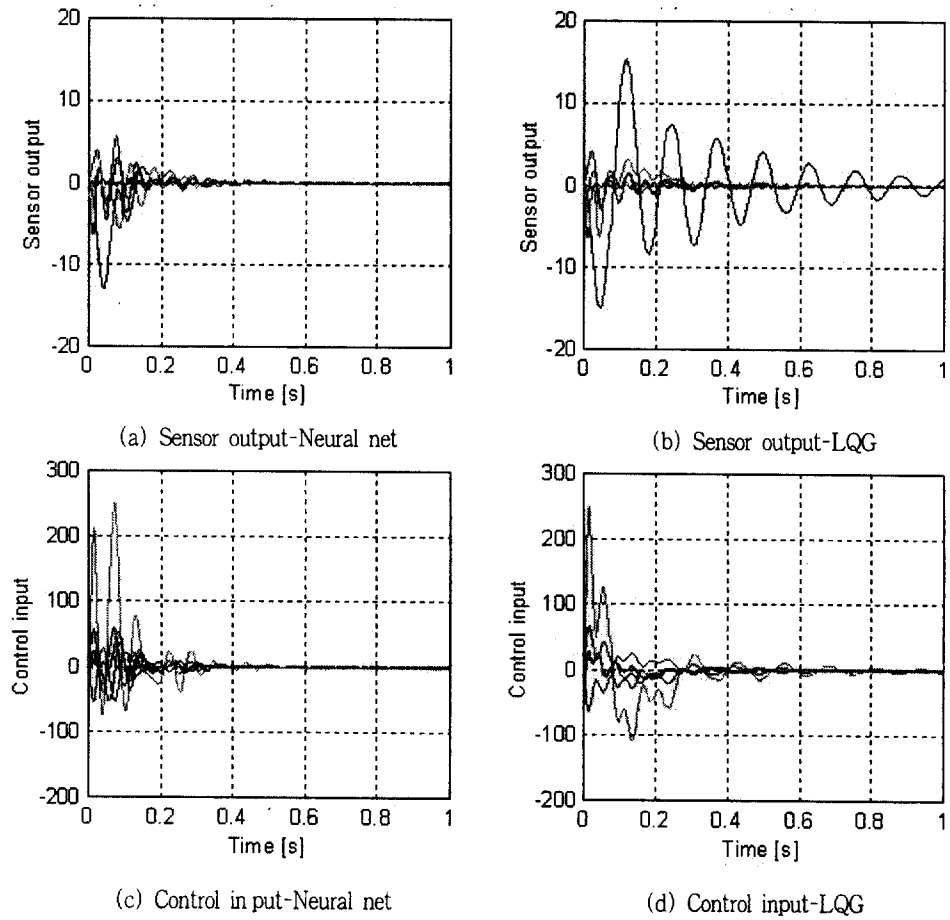

(a) Sensor output-Neural net

(b) Sensor output-LQG

(c) Control in put-Neural net

(d) Control input-LQG

Fig. 12. Comparison of the trained neural net control input with the LQG control input

V. Conclusion

Our recent development in a smart structure module and its integration with ASTROS* is presented. Successful integration is achieved as a result of the uncovered thermal versus PZT analogy and the control-surface versus PZT equivalence principle. The smart structure module is also integrated with the ASE module of ASTROS*/ASE, through a state-space aeroservoelastic equation formulation.

For demonstration of the integrated software capability, the active flutter suppression based on the LQG and the neural net was designed for a modeled F16 Wing using PZT actuators. The PZT actuators with a proposed control system enable to stabilize all unstable modes, whereas wing flutter occurs for an open-loop system.

References

[1] T. A. Weisshaar, Aeroservoelastic Control Concepts with Active Materials, *1994 International Mechanical Engineering Congress and Exposition*, Chicago, IL, Nov., 1994.

[2] A. Suleman, V. B. Venkayya, Flutter Control of Adaptive Composite Panel, AIAA Pa-

per No. 94-1744, *Proceedings of the AIAA/ ASME Adaptive Structures Forum*, SC, April, 1994.

[3] J. Heeg, Analytical and Experimental Investigation of Flutter Suppression by Piezoelectric Actuation, *NASA TP-3241*, Feb., 1993.

[4] C. Nam, Y. Kim, Optimal Design of Adaptive Composite Lifting Surface for Flutter Suppression, *AIAA Journal*, vol. 33, no. 10, 1994, pp. 1897-1904.

[5] C. Nam, Y. Kim and T. A. Weisshaar, Optimal Sizing and Placement of Piezo Actuators for Active Flutter Suppression, *Proceedings on the Smart Structures and Materials 95. SPIE*, San Diego, CA, 1995.

[6] C. Nam, Y. Kim, K. Lee, Optimal Wing Design for Flutter Suppression with PZT Actuators Including Power Requirement, AIAA Paper No. 96-3984, *Proceedings on the 6th AIAA/ USAF/ NASA/ISSMO Symposium on Multidisciplinary Analysis and Optimization*, Bellevue, WA, 1996.

[7] C. Nam, Kim, Y. Robust Controller Design of a Wing with Piezoelectric Materials for Flutter Suppression, *10th VPI and SU Symposium on Structural Dynamics and Control*, Blacksburg, VA, 1995.

[8] J. Heeg, A. McGowan, E. Crawley and C. Lin, The Piezoelectric Aeroelastic Response Tailoring Investigation: A Status Report, *Proceedings on Smart Structures and Materials 95*, SPIE, San Diego, CA, 1995.

[9] S. Zhou, C. Liang and C. A. Rogers, Coupled Electro-mechanical Impedance Modeling to Predict Power Requirement and Energy Efficiency of Piezoelectric Actuators Integrated with Plate-like Structures, AIAA Paper No. 94-1762, *Proceedings of the AIAA/ ASME Adaptive Structures Forum*, SC, April, 1994.

[10] V. Giurgiutiu, C. A. Rogers, and R. Rusovici, Power and Energy Issues in the Induced-Strain Actuation for Aerospace Adaptive Control, Paper No. 96-1300, *Proceedings of the AIAA/ASME/AHS Adaptive Structures Forum*, UT, April, 1996.

[11] E. H. Johnson, and V. B. Venkayya, Automated Structural Optimization System(ASTROS), *Theoretical* Manual, AFWAL-TR-88-3028, vol. 1, December 1988.

[12] P. C. Chen, D. Sarhaddi, D. D. Liu and M. Karpel, A Unified AIC Approach for Aeroelastic/Aero-servoelastic and MDO Applications, *AIAA Paper* No. 97-1181-CP, to appear in Journal of Aircraft.

[13] P. C. Chen, D. D. Liu, D. Sarhaddi, A. G. Striz, D. J. Neill, and M. Karpel, Enhancement of the Aeroservoelastic Capability in ASTROS, STTR Phase I Final Report, WL-TR-96-3119, Sep., 1996.

[14] P. C. Chen, D. Sarhaddi, and D. D. Liu, A Unified Unsteady Aerodynamic Module for Aeroelastic and MDO Application, AGARD Structured and Material Panel (SMP) Workshop 2 Numerical Unsteady Aerodynamics and Aeroelastic Simulation, Alborg, Denmark, Oct., 13-17, 1997.

[15] P. F. Lichtenwalner, G. R. Little, L. E. Pado and R. C. Scott, Adaptive neural control for active flutter suppression, *ASME 1996 IMEC & E Conference Proceedings*, 1996.

[16] P. F. Lichtenwalner, G. R. Little and R. C. Scott, Adaptive neural control of aeroelastic response, *Proceedings of the SPIE, 1996 Symposium on Smart Structures and Materials*, 1996.

[17] L. E. Pado and P. F. Lichtenwalner, Neural predictive control for active buffet alleviation, AIAA-99-1319, pp.1043-1053, 1999.

[18] C. S. Ku and P. Hajela, Optimized neural network based controller for a nonlinear aero-

elastic system, AIAA-97-1182, pp.1286-1296, 1997.

[19] G. Vanderplatts, MICRO-DOT Users Manual Version 1.0, Engineering Design Optimization Inc., Santa Barbara, CA, 1985.

[20] A. Karpel, Extension to the Minimum-State Aeroelastic Modeling Method, *AIAA Journal*, vol. 29, no. 11, 1991, pp. 2007-2009.

[21] E. F. Crawley and E. H. Anderson, "Detailed Models of Piezoceramic Actuation of Beams", *Proceedings of the AIAA/ASME Structures, Structural Dynamics and Materials Conference*, pp. 2000-2010, 1989.

[22] C. A. Rogers, C. Liang and C. R. Fuller, Modeling of shape memory alloy hybrid composites for structural acoustic control, *J. Acoustical Society of America*, vol. 89, no. 1, pp.210-220, 1991.

[23] D. WSparks., Jr, Magh Neural networks for rapid design and analysis, AIAA-98-1779, 1998.

[24] R. M. Kolony, Unsteady Aeroelastic Optimization in the Transonic Region, *AIAA Paper* no. 96- 3983.

김 종 선(金鍾璿)

1961년 3월 26일 생
1983년 : 서울대학교 기계공학과 (공학사)
1985년 : 한국과학기술원 기계공학과(공학석사)
1989년 : 한국과학기술원 기계공학과(공학박사)
1989년 9월~1992년 2월 : 금오공과대학교 정밀기계공학과 조교수
1992년 3월~현재 : 한국항공대학교 항공우주 및 기계공학부 부교수
1999년 7월~2000년 6월 : Arizona State University 방문교수
관심분야 : 메카트로닉스, 강인제어, 지능구조물, 수송기계 제어

남 창 호(南昌浩)

1983년 : 서울대학교 항공공학과 (공학사)
1985년 서울대학교 항공공학과 (공학석사)
1990년 미국 Purdue University (공학박사)
1990년 9월 ~ 1992년 2월 : 국방과학연구소 선임연구원
1992년 9월~1999년 12월 : 한국항공대학교 항공우주 및 기계공학부 부교수
1998년 1월~1999년 12월 : Arizona State University 방문교수
2000년 1월~현재 : ZONA Technology Inc. 책임연구원
관심분야 : 공탄성, 지능구조물, 플러터 제어